

PAPER • OPEN ACCESS

## A Preliminary Study of a Graphene Fractal Sierpinski Antenna

To cite this article: Alberto Boretti *et al* 2020 *IOP Conf. Ser.: Mater. Sci. Eng.* **840** 012003

View the [article online](#) for updates and enhancements.

# A Preliminary Study of a Graphene Fractal Sierpinski Antenna

**Alberto Boretti<sup>1,\*</sup>, Lorenzo Rosa<sup>2,3</sup>, Jonathan Blackledge<sup>4,5,6</sup>, Stefania Castelletto<sup>7</sup>**

<sup>1</sup>Department of Mechanical Engineering, College of Engineering, Prince Mohammad Bin Fahd University, Al Khobar, Saudi Arabia

<sup>2</sup>Department of Engineering “Enzo Ferrari”, the University of Modena and Reggio Emilia, Modena, Italy

<sup>3</sup>Applied Plasmonics Lab, Centre for Micro-Photonics, Swinburne University of Technology, Hawthorn, Victoria, Australia

<sup>4</sup>School of Electrical and Electronic Engineering, Technological University Dublin, Ireland

<sup>5</sup>Faculty of Science and Technology, University of Wales, Wrexham, United Kingdom

<sup>6</sup>Department of Computer Science, University of Western Cape, Cape Town, South Africa

<sup>7</sup>School of Engineering, RMIT University, Bundoora, Victoria, Australia

\*Email: a.a.boretti@gmail.com

**Abstract.** We provide a preliminary study of a Graphene fractal antenna operating at THz frequencies with the opportunity to modulate the emission. There are many advantages of the fractal design, namely multiband/wideband ability, and, a smaller, lighter and simpler configuration for higher gain, that can benefit from the coupling with Graphene, the thinnest and strongest of materials exhibiting very high electrical conductivity and tunability. This paper proposes a conceptual background for the study and presents some preliminary results on the electromagnetic emission simulations undertaken.

## 1. Introduction

Fractal antennas are receiving attention for the future of wireless communication because of their wideband and multiband capabilities, the opportunity of fractal geometries to drive multiple resonances and the ability to make smaller and lighter antennas, with fewer components and radiative elements less circuitry and higher gains. Extremely small and extremely high-frequency nanometric fractal antennas based on Graphene, a one-atom-thick, two-dimensional carbon crystal, may enhance wireless communications for commercial and military applications.

Nanoantennas based on surface plasmon polaritons enable the conversion of light from free space into sub-wavelength volumes establishing a way of communication using free-electron propagation within networks of nanosized devices. This approach can be of high impact for many applications, including biochemical sensors, reconfigurable meta-surfaces, compact optoelectronic devices, advanced health monitoring, drug delivery systems and wireless nano-sensor networks for biological and chemical attack prevention. Dynamic control and reconfigurable properties of these antennas are also very desirable for the above applications. Owing to its unique electronic properties, Graphene has recently been identified as a promising platform to build integrated active plasmonic nanoantennas for a wide wavelength range in the mid-infrared, i.e. 10 - 100 THz.

A Graphene fractal antenna is regarded as a high-frequency tunable antenna for radio communications in the Terahertz bandwidth, enabling unique applications in the military field, such as wireless nanosensor networks for biological and chemical attack prevention. Graphene is a one-atom-



thick two-dimensional allotrope of Carbon [1], with the highest known electrical conductivity that is currently unavailable in any other materials, including metals such as gold and silver. The nanostructures of Graphene can enable wireless communication enhancements within nanoscale electronic devices with a significant reduction in the energy needed for such communications [2]. Furthermore, as the electrons oscillate, they create an electromagnetic wave on top of the Graphene layer, referred to as the Surface Plasmon Polariton (SPP) wave [3], [4]. This enables the antenna to operate at the lower end of the Terahertz frequency spectrum [5], [6], which can be more efficient than current copper-based antennas [7].

In this paper, we study a Sierpinski fractal triangle monopole antenna made of gold, graphene, silicon, and silicon dioxide by solving Maxwell's equation for a complex refractive index in the frequency domain over the range 10 - 700 THz [8]. A few layers of graphene are deposited on a nanometric layer of silica on a Si substrate. Every material in the nanostructure is modeled through the complex refractive index with real,  $n$ , and, imaginary parts,  $k$ . The values of  $n$  and  $k$  are obtained from experimental data and theoretical models. The design permits the application of a gate voltage to modify the graphene optical conductivity over the operating region of 10 - 300 THz. We compare this design in Graphene and the operation with different gate voltages to the same design in gold, identifying the differences of using Graphene under the influence of the gate voltage.

The present dimensions follow the computational constraints set up by the thickness of the fractal that cannot be thicker than 3 nm. A better design for the fractal antenna is to scale it up by an order of magnitude or more while retaining the same thickness. This can be investigated as soon as such a design is feasible. Such a design will be able to scan with an order of magnitude smaller frequencies (10 times larger wavelengths). In this work, we model the material properties for wavelengths of 30 - 0.4  $\mu\text{m}$  (10 -750 THz).

Our approach differs from similar work in [9], for example, where Graphene is placed underneath a Copper patch and the fractal is on the 100 x 100  $\mu\text{m}$  scale. Here, we consider a design that extends the frequency range of operation of a fractal antenna by introducing nanofeatures. Further, Graphene nanoantenna plasmonic properties [3], [6], [10] provide tunability in the Terahertz domain due to the Graphene surface conductivity, that can be modified by applying an electrostatic bias, which changes the chemical potential (Fermi level). In [10], Graphene is used as an electrically tunable load in a nanoscale metal antenna gap. This permits an in-situ control of the antenna's frequency. The Graphene patch antenna resonance frequency changes with its width and Sierpiński-type fractals are of growing interest because of their broadband capabilities for applications using plasmonic metallic materials which generate emissions in the optical frequency (40 - 750 THz), [11].

In this paper, the combination of Graphene plasmonics and Sierpiński-type fractals is studied for the first time for a broad-band Terahertz antenna with a focus on nanoelectronic wireless communications, [3]. We note that the combination of metallic structures and Graphene, which has gate-voltage dependent optical properties, has already provided an antenna with narrower frequency operations, tuneable between 35 and 75 THz, [10].

We aim to design a compact structure while pushing the order of the Sierpiński fractal to a high level by engineering nanometric details in Graphene. This fabrication can be achieved by Electron Beam Lithography patterning or 3D nano-patterning using focused ion beam lithography, as described in [6] and [11]. Graphene is transferred on a  $\text{SiO}_2$  substrate to control the size and features at the nanoscale. The nanoantenna is based on the Sierpiński gasket fractal, with equilateral triangles as building blocks.

## 2. Materials and methods

We simulate the optical properties of Graphene nanoantennas and the electric field intensity distribution at different resonance frequencies in the mid-infrared and the visible range. This is based on using the well-established Graphene optical conductivity based on a Drude-like model known as Kubo's formula [12], [13], within the random phase approximation in the local limit adopted by [10]. Other quantum mechanical models have recently been introduced to describe Graphene surface conductivity [14]. However, based on the recent agreement between the semi-classical model and experimental results as

given in [10], we argue that our model is a good represents of the proposed design. Additionally, we model the refractive index of Graphene in the visible range by using the experimental data from [15].

The optical or surface conductivity of Graphene is based on a semi-classical model of conductivity. The surface conductivity for a single layer of Graphene has been determined by [13] and is given by

$$\sigma_s = \sigma_{s,intra} + \sigma_{s,inter} \quad (1)$$

where

$$\sigma_{s,intra} = \frac{je^2k_B T}{\pi\hbar^2(\omega+j2\Gamma)} \left[ \frac{\mu_C}{k_B T} + 2 \ln \left( e^{-\frac{\mu_C}{k_B T}} + 1 \right) \right] \quad (2)$$

$$\sigma_{s,inter} = \frac{je^2}{4\pi\hbar} \ln \left[ \frac{2|\mu_C|-(\omega+2\Gamma)}{2|\mu_C|+(\omega+2\Gamma)} \right], \quad k_B T \ll \mu_C \quad (3)$$

In the above equations,  $\mu_C$  is the chemical potential (Fermi energy), which depends on the charge carrier concentration,  $\Gamma$  is the scattering rate with  $\tau=1/2\Gamma$  being the carrier relaxation lifetime,  $k_B$  is the Boltzmann constant,  $T$  is the temperature and  $\omega$  is the angular frequency. The first term of Eq. (1) is attributed to intra-band transitions and the second term to inter-band transitions. When the Fermi level is below half of the photon energy ( $E_{ph} = \hbar\omega$ ), the contribution from the inter-band transition (visible and UV domain) dominates the optical conductivity. The inter-band surface conductivity can be calculated numerically or given in the analytic form under certain approximations. Once the Fermi level is increased above half of the photon energy, interband transitions are diminished due to Pauli blocking and intra-band transitions (in the IR and mid-IR) play a dominant role. To generate the surface conductivity of Graphene, the intra-band conductivity term can be obtained analytically while the inter-band conductivity term needs to be determined numerically.

A Drude-like approximation for  $\sigma_s$ , is valid for mid-infrared wavelengths, where the intra-band conductivity term usually dominates over the inter-band term; thus, an approximation can be obtained from Eq. (2) for 0.01 to 100 THz given by

$$\sigma_{s,intra} \approx \frac{je^2\mu_C}{\pi\hbar^2(\omega+j2\Gamma)} \quad (4)$$

where the carriers relaxation time is  $\tau^{-1} = \frac{ev_f^2}{\mu\mu_C}$ ,  $\mu$  being the carrier mobility which is typically 2,000  $\text{cm}^2/(\text{V s})$  and  $v_f$ , the Fermi velocity of Dirac fermions in Graphene is given by  $v_f \approx 8.5 \times 10^5 \text{ ms}^{-1}$  to  $3 \times 10^6$ . With a silica substrate, a measured value can be found which is  $1.8 \times 10^6$ , [16].

A specific conductivity model was derived in [3], by taking into account the impact of lateral electron confinement in Graphene nanoribbons, but the above models converge for Graphene strips which are 50 nm wide or more. Further, experimentally measured values of the surface conductivity of Graphene nanoribbons can be utilized to better model small nanofeatures [17]. A closed empirical expression [18] that resolves numerical singularities in the Graphene surface conductivity occurring at  $\hbar\omega = 2\mu_C$  can also be used for  $\lambda > 250 \text{ nm}$  up to a few microns; this model provides comparable results to the model adopted here, at least in the visible spectrum.

In this paper, we consider the Graphene sheet optical conductivity within the Random-Phase Approximation (RPA) in the local limit [12], [19] and also adopted in [10]. This model has been validated against direct measurements of the Graphene bulk conductivity. According to this model, the surface optical conductivity is given by

$$\sigma_s(\omega) = \frac{2je^2k_B T}{\pi\hbar^2(\omega+2\Gamma)} \ln \left[ 2 \cosh \frac{\mu_C}{2k_B T} \right] + \frac{e^2}{4\hbar} \left[ \frac{1}{2} + \frac{1}{\pi} \arctan \left( \frac{\hbar\omega-2\mu_C}{2k_B T} \right) \right] - \frac{j}{2\pi} \ln \frac{(\hbar\omega+2\mu_C)^2}{(\hbar\omega-2\mu_C)^2+(2k_B T)^2} \quad (5)$$

where the first term is attributed to the intra-band transition and the second term is the inter-band transition. The Graphene Fermi level,  $\mu_C$ , can be changed by applying a gate voltage. The approximate relationship can be estimated as a parallel capacitor. The capacitor-induced carrier concentration of the

Graphene is  $n_g = \epsilon_0 \epsilon_d V_g / ed$  and the Fermi level is  $\mu_C = \hbar v_f (\pi n_g)^{1/2}$ . Here the  $\epsilon_d$  is the dielectric constant of the insulating layer and  $d$  is the thickness of the insulating layer.

The bulk conductivity is related to the surface conductivity by  $\sigma_V = \frac{\sigma_s}{\Delta}$ , where  $\Delta$  is the thickness of the Graphene layer, which is much smaller than the excitation wavelength. In this context, Graphene is modeled as a very thin (< 4nm) three-dimensional material. The volumetric anisotropic permittivity,  $\epsilon$ , can then be calculated if we assume that the Graphene layer has a finite thickness,  $\Delta$ .

To turn the surface conductivity of a Graphene layer into a uniaxial anisotropic permittivity, the background relative permittivity of a thick material (Graphite),  $\epsilon_r$ , is introduced. The uniaxial anisotropic permittivity, in-plane and out of the plane components are then given by [20]

$$\epsilon_{\parallel} = \epsilon_r + j \frac{\sigma_s}{\epsilon_0 \omega \Delta} \quad (6)$$

$$\epsilon_{\perp} = \epsilon_r$$

where  $\epsilon_r$  can be set at 2.5, [20] which is based on the dielectric constant of Graphite. The real and imaginary refractive index components can then be obtained from  $\mathbf{n} + i\mathbf{k} = \sqrt{\epsilon_{\parallel}}$ .

### 3. Results

Preliminary simulations are performed for a 3<sup>rd</sup>-order Sierpinski fractal monopole antenna of nanometric dimensions. The Graphene fractal triangle has lateral dimensions 640 nm x 560 nm and a thickness of 3 nm. The smallest triangle from which the fractal is composed has lateral dimensions 1/16 times the 'fundamental triangle'. The fractal triangle is deposited on top of a 10 nm SiO<sub>2</sub> substrate which rests on top of a 10 nm Si substrate. The fractal antenna is fed by a coaxial cable and placed on a ground plane that has a diameter of 800 nm and a thickness of 25 nm. This is the basic configuration.

Macroscale Sierpinski fractal triangle monopole antennas are intended to be used for different discrete frequency bands. Nanoscale equivalent antennas are not expected to operate in the same way, as the materials have their properties and cannot be assimilated to be a Perfect Electric Conductor (PEC). At the nanoscale, the volumetric conductivity is described in terms of the real and imaginary components of the relative permittivity, which can be translated in terms of the real (n) and imaginary (k) components of the refractive index.

In the model, a Graphene fractal is connected through a coaxial lumped port to a ground plane made of gold. One spherical Perfectly Matched Layer (PML) then includes the Sierpinski fractal triangle, the ground plane and the surrounding volume of air. The bottom of the Sierpinski fractal triangle is flat and connected to the coaxial cable feed. The inner coaxial cable is taken to be gold and surrounded by a SiO<sub>2</sub> outer coaxial casing. In our simulations, the ground plane is also made of gold and the Sierpinski fractal triangle made of Graphene.

As Graphene is two-dimensional material, the volumetric conductivity is expressed in terms of the surface conductivity divided by the Graphene layer thickness as described in Eq. (7). The Sierpinski fractal triangle is positioned on a layer of a dielectric SiO<sub>2</sub> on top of a semiconductor Si substrate. Additional matching parts are not required for using the antenna at higher-order resonances with the given fractal structure. The governing equation for the propagation of electromagnetic waves in the (temporal) frequency domain is obtained from Maxwell's equation and given by

$$\nabla \times (\nabla \times \mathbf{E}) - k_0^2 \epsilon_r \mathbf{E} = \mathbf{0} \quad (7)$$

$$\epsilon_r = (\mathbf{n} - i\mathbf{k})^2$$

For the lumped port, the governing equation is  $Z = V_1 / I_1$ .

The temporal frequency domain model is appropriate under the assumption that all material properties are constant for field strength and that the field will change sinusoidally in time over the range of frequencies considered. The properties of the materials do not play any role in the macroscopic model, providing the conductivity is high enough to qualify as PEC. However, at the nanoscale, the material models for n and k selected in the design change the resonances of the antenna. For the nanometric

dimensions, and, given fractal antenna theory the macroscopic Sierpinski, the second and third-order resonances of the small structures are placed at 320 and 600 THz [8]. We study the small structure for 10 -1000 THz.

Concerning the material properties, for the case of Gold, experimental values for  $n$  and  $k$  are provided for different configurations (films of different thickness, evaporated gold, template stripped gold, single-crystal gold) over the range of wavelength 0.3-25  $\mu\text{m}$  [21], [22]. For Silicon, the  $n$ ,  $k$  data are obtained over the range 0.2-1.45  $\mu\text{m}$  from [23] and [24]. Above this wavelength, the values are extrapolated linearly. For Silicon Dioxide, the  $\text{SiO}_2$  values of  $n$  and  $k$  are available for 0.21 – 1000  $\mu\text{m}$  from [25]. In the case of Graphene, experimental measurements of  $n$  and  $k$  are available in the region 0.15-0.95  $\mu\text{m}$  from [15]. These values depend on the Graphene thickness and substrate. Alternatively Graphene surface conductivity is modeled using the RPA in the local limit [12] from Eq. (6), based on validation of the carrier relaxation time measured from the Graphene bulk conductivity at 300 K [10].

Figure 1 presents the model for real and imaginary components of the Graphene relative permittivity, refractive index, and surface conductivity obtained using the RPA in the local limit (Eq. 6) with  $\mu_c=0.43$  eV, corresponding to a carrier concentration of  $n_g = 1.1 \times 10^{17}$  and  $\mu_c=0.19$  eV ( $V_g=2.5\text{V}$ ), corresponding to a carrier concentration of  $n_g = 2.2 \times 10^{16}$   $\text{m}^{-2}$  ( $V_g=0.5\text{V}$ ). Graphene has the advantage of tunability, i.e. the opportunity of changing  $n$ ,  $k$  by applying a voltage across the thin layer, as this introduces a change on the Fermi energy level ( $\mu_c$ ) and thus of the carrier concentration,  $n_g$ . This gives the ability to reconfigure the frequencies of the antenna. Thus, we used values of carrier mobility of  $\mu = 2000$   $\text{cm}^2/(\text{Vs})$ ,  $v_f=1.2 \times 10^6$   $\text{ms}^{-1}$  and  $\mu_c=0.19$  eV and 0.43 eV, corresponding to a carrier concentration of  $n_g = 2.2 \times 10^{16}$   $\text{m}^{-2}$  and  $1.1 \times 10^{17}$   $\text{m}^{-2}$ , respectively.

Assuming a  $\text{SiO}_2$  of thickness  $d=10$  nm, it takes  $V_g \sim 0.5 - 2.5$  V to change the Fermi level from 0.19 - 0.43 eV. These values are used to match the experimental validation of a Graphene single layer surface conductivity measurements reported in [10]. The real and imaginary parts of the refractive index of Graphene can be obtained from the surface optical conductivity model as described in Eq. (6) and the volumetric anisotropic permittivity as given in Eq. (7). This model is validated from 3 to 10  $\mu\text{m}$  and can be extended to lower wavelengths. The application of a voltage across the Graphene layer is not modeled, but values of  $n$  and  $k$  are modified accordingly.

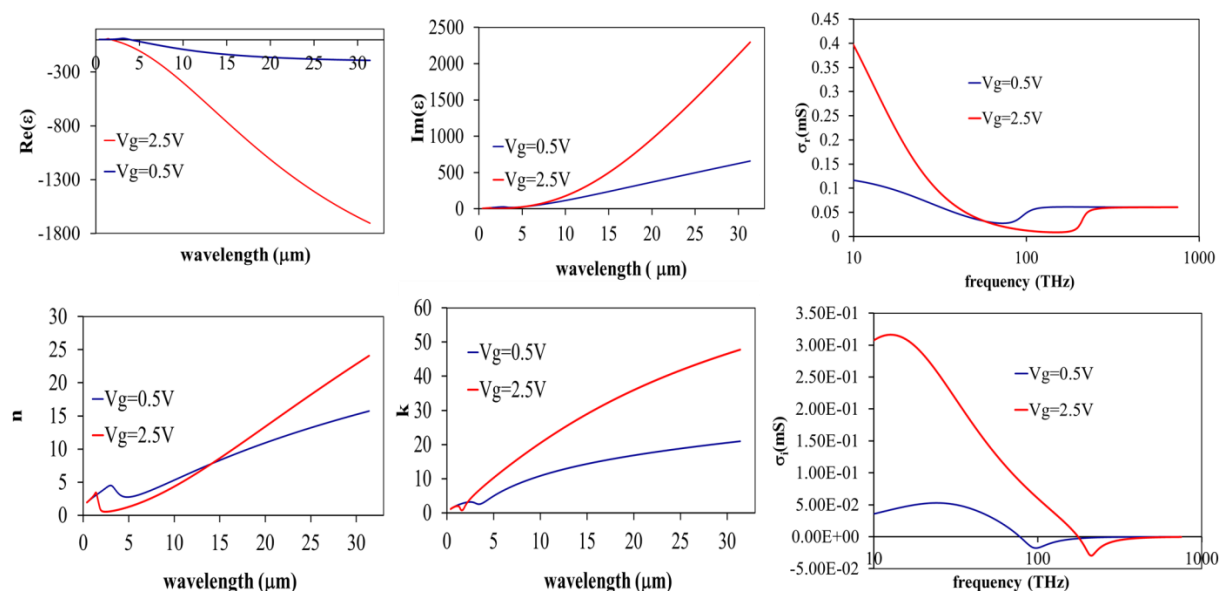
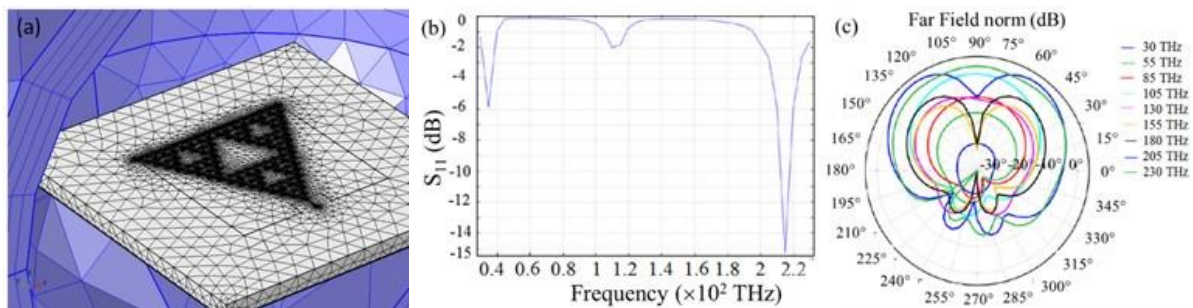


**Figure 1.** Model for the real and imaginary components of the Graphene relative permittivity  $\epsilon$ , refractive index ( $n$ ,  $k$ ) and surface conductivity ( $\sigma_r$ ,  $\sigma_i$ ) obtained using the RPA in the local limit (Eq.6) with  $\mu_c=0.43$  eV, corresponding to a carrier concentration of  $n_g = 1.1 \times 10^{17}$   $\text{m}^{-2}$  (red lines) and  $\mu_c=0.19$  eV ( $V_g=2.5\text{V}$ ), corresponding to a carrier concentration of  $n_g = 2.2 \times 10^{16}$   $\text{m}^{-2}$  ( $V_g=0.5\text{V}$ ) (blue lines)

Example results of our simulations are given in Figure 2. In this simplified model, the far-field emission is similar to the one that could be achieved by a radiator modeled as a PEC. However, lower resonance frequencies are observed due to the properties of the material. From actual nanometric dimensions but with classic macroscopic Sierpinski fractal antenna theory, second and third-order resonances of the structure are placed at 320 to 600 THz. Depending on the values of  $n$  and  $k$  for the actual material selected for the fractal radiator the ground plane and inner coaxial, this pattern is changed at the nanoscale as observed in the results given in Figure 2(c). In this case, three resonances are found at 35, 110 and 215 THz.

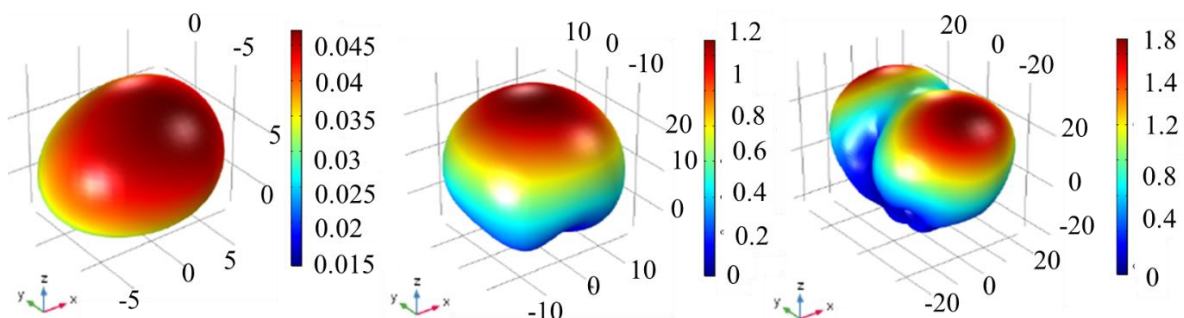
Current dimensions are dictated by the thickness of Graphene being less than 3 nm. The thickness of Graphene also influences the tunability. This dictates the minimum size of the mesh for modeling the fractal which must be a fraction of the thickness. To keep the number of mesh elements to a minimum, the other dimensions have also been kept to a minimum; hence, the 10 - 1000 THz range, as shown in Figure 2. By further scaling the antenna to operate in the range of frequency 10 - 120 THz,

Graphene may have the advantage of being able to tune the refractive index (surface conductivity) if the thickness is approximated to a single layer or a few layers, by applying a voltage across the layer and substrates. As discussed in [26], the opportunity to model the properties of Graphene given a suitable Maxwell equations solver relies on special conditions to be enforced for the current density within the radiator. This can be accomplished by evaluating the complex permittivity of Graphene as the frequency and other parameters are varied and treating the film thickness as an impedance boundary that establishes a relationship between the currents flowing on the two film surfaces. This increases the number of degrees of freedom and computational complexity, but, in this way, the total losses through the film can be computed with a more computationally stable discretization. Moreover, nanoscale effects such as interface roughness can be introduced, evaluated, and correlated with experimental evidence. Hence, back-to-back modeling and experimental activity are certainly necessary to further progress the design.



(d) 3D Radiation patterns at different frequencies

Frequency 35 THz	Frequency 110 THz	Frequency 215 THz
D=3.95 dB	D=8.18 dB	D=8.34 dB



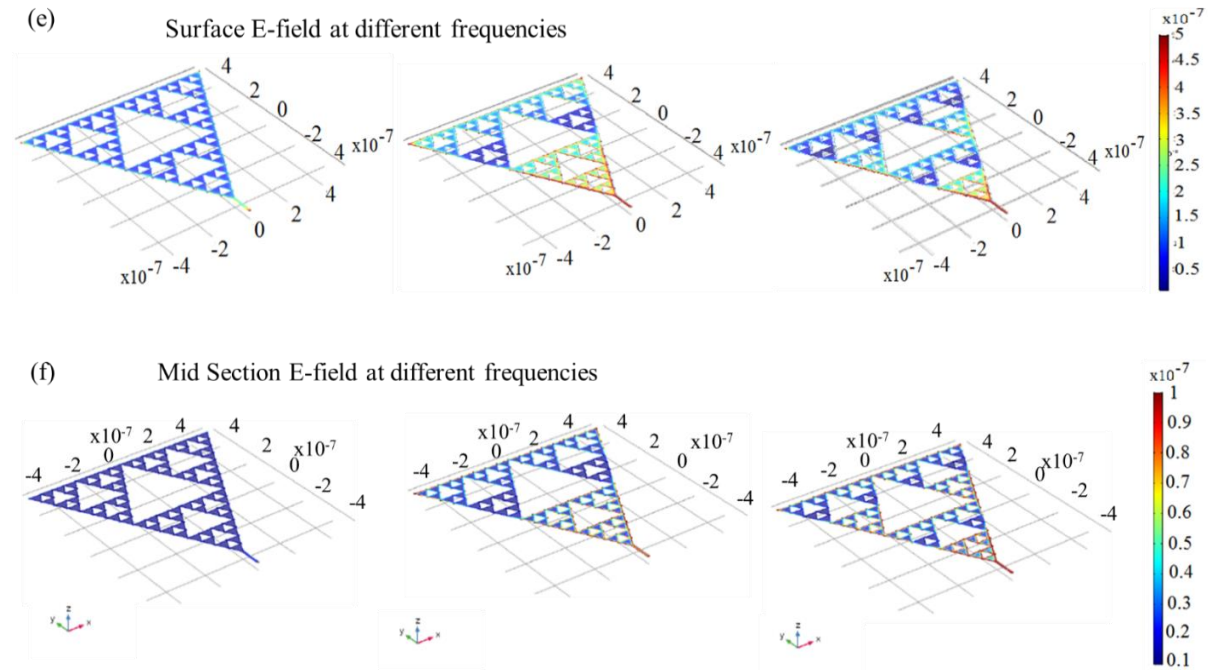


**Figure 2.** (a) Sierpinski antenna model. (b) Sierpinski Global S-parameter (in dB) vs. frequency with three resonances at 35, 110 and 215 THz. (c) Sierpinski far-field polar coordinate patterns at selected frequencies. (d) 3D emission patterns. (e) Sierpinski surface E-fields at the resonance frequencies. (f) Sierpinski mid-section E-fields at the resonance frequencies.

#### 4. Conclusions

A preliminary study has been performed for a Graphene fractal antenna to work in the THz frequencies with the opportunity to modulate the emission. The paper has proposed the conceptual background for the study, as well as the result of simulations based on the Maxwell equations (Eq. 8). The model must be carefully revised to simulate the proposed antenna by using externally performed simulations for the conditions to be enforced in the Maxwell solver.

#### 5. References

- [1] Geim, A.K.; Novoselov, K.S. The rise of graphene. *Nat Mater* 2007, *6*, 183-191.
- [2] Wang, Z.L. Towards self-powered nanosystems: From nanogenerators to nanopiezotronics. *Advanced Functional Materials* 2008, *18*, 3553-3567.
- [3] Jornet, J.M.; Akyildiz, I.F. Graphene-based plasmonic nano-antenna for terahertz band communication in nanonetworks. *IEEE Journal on Selected Areas in Communications* 2013, *31*, 685-694.
- [4] Ju, L.; Geng, B.; Horng, J.; Girit, C.; Martin, M.; Hao, Z.; Bechtel, H.A.; Liang, X.; Zettl, A.; Shen, Y.R., *et al.* Graphene plasmonics for tunable terahertz metamaterials. *Nat Nano* 2011, *6*, 630-634.
- [5] Llatser, I.; Kremers, C.; Cabellos-Aparicio, A.; Jornet, J.M.; Alarcón, E.; Chigrin, D.N. Graphene-based nano-patch antenna for terahertz radiation. *Photonics and Nanostructures - Fundamentals and Applications* 2012, *10*, 353-358.
- [6] Zakrajsek, L.; Einarsson, E.; Thawdar, N.; Medley, M.; Jornet, J.M. Lithographically defined plasmonic graphene antennas for terahertz-band communication. *IEEE Antennas and Wireless Propagation Letters* 2016, *15*, 1553-1556.
- [7] Dragoman, M.; Muller, A.A.; Dragoman, D.; Cocchetti, F.; Plana, R. Terahertz antenna based on graphene. *Journal of Applied Physics* 2010, *107*, 104313.

- [8] Mishra, R.K.; Ghatak, R.; Poddar, D.R. Design formula for sierpinski gasket pre-fractal planar-monopole antennas [antenna designer's notebook]. *IEEE Antennas and Propagation Magazine* 2008, *50*, 104-107.
- [9] Xu, Y.Y.; Xu, Y.; Hu, J.; Yin, W.Y. In *Design of a novel reconfigurable sierpinski fractal graphene antenna operating at thz band*, 2013 IEEE Antennas and Propagation Society International Symposium (APSURSI), 7-13 July 2013, 2013; pp 574-575.
- [10] Yao, Y.; Kats, M.A.; Genevet, P.; Yu, N.; Song, Y.; Kong, J.; Capasso, F. Broad electrical tuning of graphene-loaded plasmonic antennas. *Nano Letters* 2013, *13*, 1257-1264.
- [11] Rosa, L.; Sun, K.; Juodkazis, S. Sierpin'ski fractal plasmonic nanoantennas. *physica status solidi (RRL) – Rapid Research Letters* 2011, *5*, 175-177.
- [12] Falkovsky, L.A.; Pershoguba, S.S. Optical far-infrared properties of a graphene monolayer and multilayer. *Physical Review B* 2007, *76*, 153410.
- [13] Hanson, G.W. Dyadic green's functions and guided surface waves for a surface conductivity model of graphene. *Journal of Applied Physics* 2008, *103*, 064302.
- [14] Firsova, N.E.; Yu, A.F. Quantum description of nanoantenna properties of a graphene membrane. *EPL (Europhysics Letters)* 2016, *114*, 57003.
- [15] Ochoa-Martinez, E.; Gabas, M.; Barrutia, L.; Pesquera, A.; Centeno, A.; Palanco, S.; Zurutuza, A.; Algora, C. Determination of a refractive index and an extinction coefficient of standard production of cvd-graphene. *Nanoscale* 2015, *7*, 1491-1500.
- [16] Hwang, C.; Siegel, D.A.; Mo, S.-K.; Regan, W.; Ismach, A.; Zhang, Y.; Zettl, A.; Lanzara, A. Fermi velocity engineering in graphene by substrate modification. 2012, *2*, 590.
- [17] Han, M.Y.; Özyilmaz, B.; Zhang, Y.; Kim, P. Energy band-gap engineering of graphene nanoribbons. *Physical Review Letters* 2007, *98*, 206805.
- [18] Simsek, E. A closed-form approximate expression for the optical conductivity of graphene. *Optics Letters* 2013, *38*, 1437-1439.
- [19] Falkovsky, L.A.; Varlamov, A.A. Space-time dispersion of graphene conductivity. *The European Physical Journal B* 2007, *56*, 281-284.
- [20] Gao, W.; Shu, J.; Qiu, C.; Xu, Q. Excitation of plasmonic waves in graphene by guided-mode resonances. *ACS Nano* 2012, *6*, 7806-7813.
- [21] Gao, L.; Lemarchand, F.; Lequime, M. Comparison of different dispersion models for single layer optical thin film index determination. *Thin Solid Films* 2011, *520*, 501-509.
- [22] Olmon, R.L.; Slovick, B.; Johnson, T.W.; Shelton, D.; Oh, S.-H.; Boreman, G.D.; Raschke, M.B. Optical dielectric function of gold. *Physical Review B* 2012, *86*, 235147.
- [23] Green, M.A. Self-consistent optical parameters of intrinsic silicon at 300k including temperature coefficients. *Solar Energy Materials and Solar Cells* 2008, *92*, 1305-1310.
- [24] Chandler-Horowitz, D.; Amirtharaj, P.M. High-accuracy, midinfrared ( $450\text{cm}^{-1} \leq \omega \leq 4000\text{cm}^{-1}$ ) refractive index values of silicon. *Journal of Applied Physics* 2005, *97*, 123526.
- [25] Kitamura, R.; Pilon, L.; Jonasz, M. Optical constants of silica glass from extreme ultraviolet to far infrared at near room temperature. *Appl. Opt.* 2007, *46*, 8118-8133.
- [26] COMSOL Webinar "Simulating Graphene-Based Photonic and Optoelectronic Devices", [cn.comsol.com/community/exchange/361/](http://cn.comsol.com/community/exchange/361/)